Identification of radiative heat transfer parameters in multilayer thermal insulation of a spacecraft

Aleksey V. Nenarokomov[1], Leonid A. Dombrovsky[2], Irina V. Krainova[1], Oleg M. Alifanov[1], Sergey A. Budnik[1]

[1] Moscow Aviation Institute, Moscow, Russia
[2] Joint Institute for High Temperatures, NCHMT, Moscow, Russia

KEY WORDS: Radiation, Thermal insulation, Identification in spectral domain, Fibrous spacer, Vacuum experiment.

Abstract
The study is motivated by necessity to optimize multilayer vacuum thermal insulation (MLI) of modern high-weight spacecraft. The modern approaches to the design of space structures assume broad application of physical models and computational methods. The latter is impossible if information on physical properties is insufficient. In many cases, both theoretical prediction and direct measurements of radiative properties of composite materials is very problematic. There is only one way to overcome these complexities. It is the use of some indirect measurements. Mathematically, such an approach is usually formulated as a solution of the inverse problem: to retrieve the properties from the measurements of thermal characteristics of the insulation. The experiments in thermo-vacuum facilities are used to re-estimate some radiative properties of metallic foil / metallized polymer foil and spacer. The specimens of a real MLI of the BP-Colombo satellite (ESA) were examined in the experiments. The retrieved values of the effective emissivity can be used directly for heat transfer calculations in the case of similar thermal conditions. Therefore, it is important to use the identified parameters to validate and improve theoretical models. The latter is considered as an objective of our further work.

1. INTRODUCTION

The present study is a part of a work on optimization of passive thermal control systems (TCS) for space vehicles. The specific of the external heating of space vehicles during the flight enables us to consider some variants of passive TCS based on screening the vehicle surface from the direct solar radiation, the solar radiation reflected by the planets, and also from thermal radiation of closely spaced planets. Various multilayer insulations (MLI) are widely used to solve this engineering problem [1]. This type of vacuum insulations has obvious advantages such as high thermal resistance at a relatively low density and convenience of their use for the surfaces of complex shape (Fig.1).

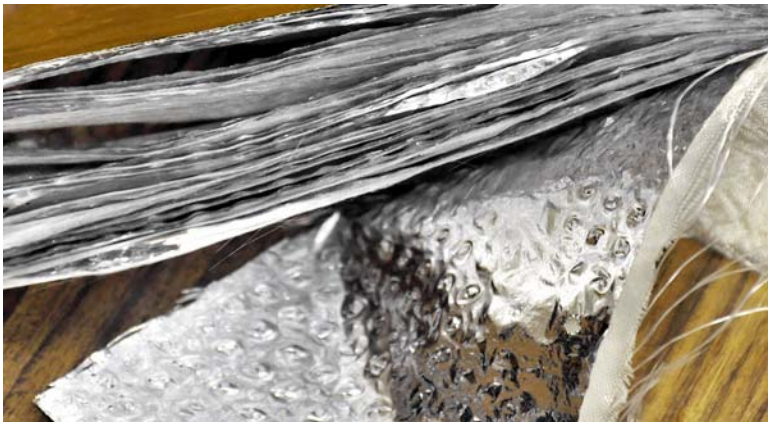

Fig. 1 A photo of the MLI sample.

A typical MLI looks as a set of thin metal screens of thickness about 5–9 μm with spacers between them. The spacer prevents a contact between the screens. Simple estimates show that the use of several layers (screens with spacers) may lead to a significant reduction of heat flux to the protected surface. MLI's with 10–30 shielding layers are usually used. The material choice for MLI depends on the expected level of temperature. The PET (polyethylene terephthalate) film coated with aluminum, silver, or gold can be used for screens at working temperatures of MLI up to 423 K. The aluminum foil with spacers of fiberglass is used at higher temperatures up to 723 K. At temperatures greater than 723 K, the foil is made of copper, nickel or steel and the spacer is made of quartz fibers. The surface density of ten screens of PET film is in the range of 0.2–0.3 kg/m^2, whereas the use of metal foils increases this value up to 1 kg/m^2 [1]. However, regardless of used materials, the principle of the MLI work is the same.

The traditional MLI thermal model [2] is very simplified. This model is based on the gray approximation and does not take into account the effects of both semi-transparent fibrous spacers between the foils and possible oxidation of aluminum foil. However the present-day computational models for radiative heat transfer in a single layer of the vacuum insulation are insufficient to solve this problem because the experimental data for the wide-range infrared radiative properties of materials are not quite reliable. Moreover, our preliminary estimates showed that the known physical effect of near-field radiative transfer between two closely spaced layers of aluminum foil may lead to a significant increase in the radiative flux. A theoretical prediction of this effect is very sensitive to the distance between the foils, and it is problematic to obtain accurate quantitative results for various flight conditions. In addition, the role of a highly-porous fibrous spacer between the foils (see Fig. 2) has been estimated in our recent papers by neglecting the near-field effect.

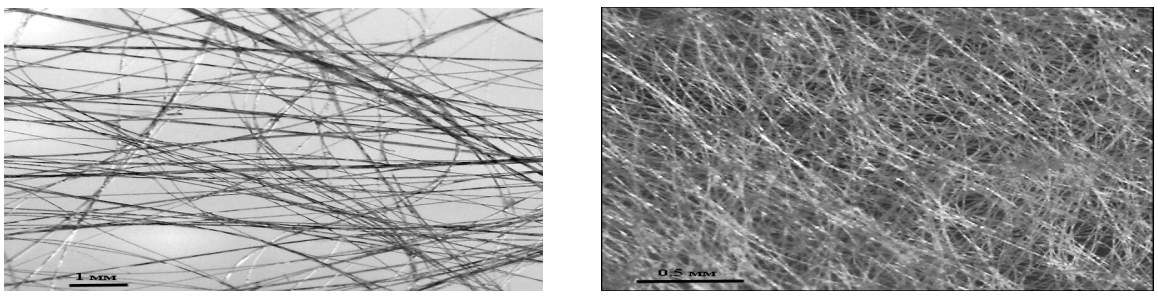

a b

Figure 2: Photographs of typical materials used for spacers between two foil layers:
a – material of a very low density, b – relatively dense material.

Obviously, the estimate of the spacer effect should be revised in a general theory taking into account a small thickness of the gap between the foils. This theoretical study is in the very beginning now. Therefore, the role of the inverse problem solution in obtaining the radiative flux at realistic conditions is considered as an important stage of the work. For brevity, we do not give here the complete mathematical problem statement, which can be found in our previous papers. At the same time, it should be noted that we are focused on identification of the conventional effective emissivity, which is the key integral parameter (over the spectrum) used to determine radiative heat transfer in the vacuum insulation of a spacecraft.

2. PHYSICAL MODEL AND EXPERIMENTAL FACILITY

The objective of the experimental study is to estimate total thermal resistance of the MLI blanket, which is a screen-vacuum thermal insulation elaborated for the temperature range from 300 to 900 K. Obviously, the accurate measurements for vacuum insulations are not simple. The space vacuum in the laboratory installation is not the only condition of successful measurements. The other problem is a very high thermal resistance of the MLI. We had no possibility to develop a specific method and use an additional facility to minimize an error of these measurements. Therefore, a previously developed vacuum installation TVS-1 is employed. Let us consider the experimental facility and the scheme of the temperature measurements. The MLI sample of size about 150×150×5 mm was placed in the experiment module EM-2 (see photo in Fig. 1 and scheme of the MLI in Fig. 3).

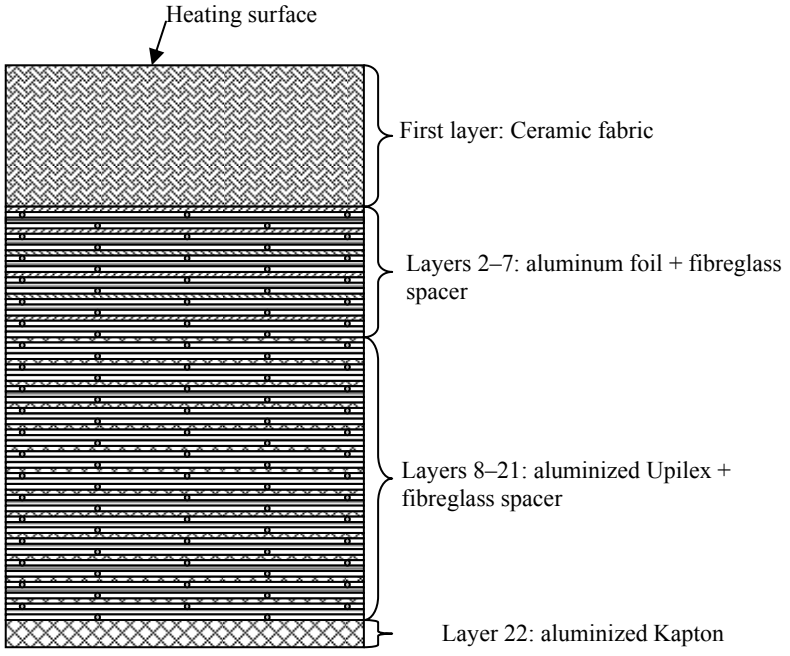

Figure 3: A scheme of the tested multilayered thermal-insulating blanket.

A scheme of temperature measurements with a set of thermocouples is presented in Fig. 4. The thermocouple T_1 is installed in the heated ceramic fabric. Two thermocouples T_6 and T_7 are installed

on the copper plate at the cold surface of sample A (T_7 is the standby thermocouple) and similar thermocouples T_8 and T_9 – in the copper plate at the cold surface of sample B (T_9 is the standby thermocouple). An electric heater made of a refractory stainless steel foil of 0.1 mm thickness is used. Elements of the insulating holder are arranged around the sample. The thermocouple conductors, covered by the glass-sleeve, are lead out through special ducts at the elements of holder. The setting frames press densely the sample in the insulating holder to the heater, and 5 mm in depth holders provide non-stress merit of the samples (preserve the initial thickness). The experimental module EM-2 is placed into a vacuum chamber of installation TVS-1. Also thermocouple T_2 is installed on the steel wall of installation cooled by water.

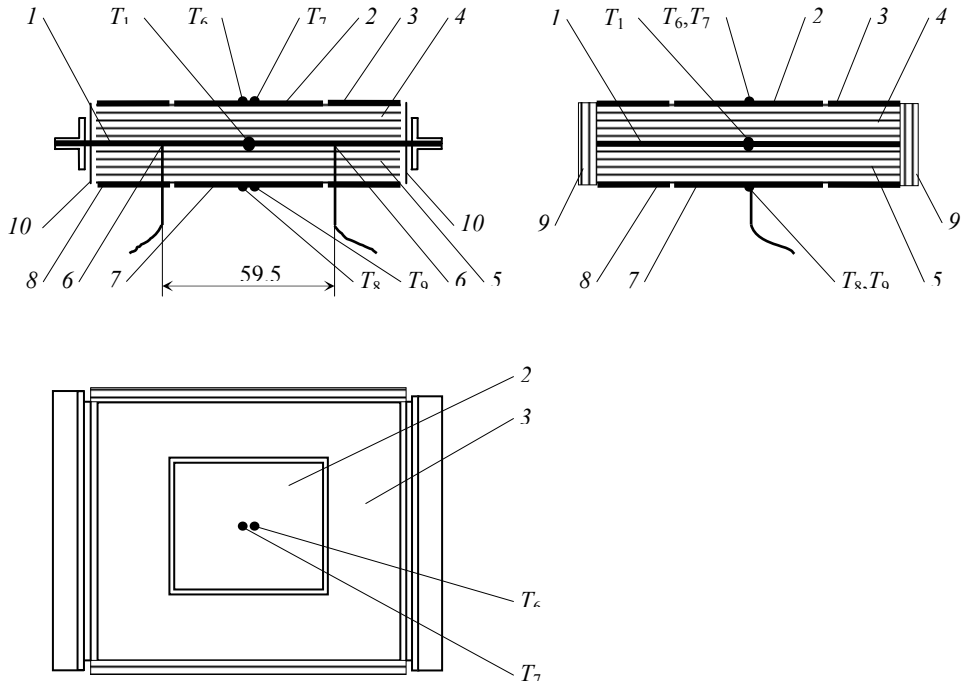

Figure 4: A scheme of temperature measurements:
1 – heating element of module EM-2 (steel foil); *2* – copper slab on specimen A; *3* – protection on specimen A; *4* – specimen A; *5* – specimen B; *6* – voltage measuring points on the heating element; *7* – copper slab on specimen B; *8* – protection of specimen B; *9* – elements of insulating holder of MLI; *10* – elements of insulating slab.

3. MATHEMATICAL MODEL

As was mentioned above, an improved theoretical model has been recently developed by the authors [3, 4]. A MLI is considered as the set of couples of screens and a spacer made of semi-transparent highly porous fibrous material between them. The resulting mathematical problem statement can be found in [4] and it is not reproduced below. At the same time, the main assumptions and special features of this approach should be briefly discussed. It was assumed that: (1) There is no any thermal contact between the screens and spacer, and thermal radiation is the only heat transfer mode to be considered; (2) The radiative flux in normal direction can be determined as a solution of a 1-D

problem neglecting small 2-D effects; (3) The isothermal metal screens are totally opaque for thermal radiation; (4) Both transmittance and reflectance of radiation by highly porous fibrous spacers can be determined on the basis of independent scattering hypothesis [5]; (5) The Mie theory for randomly oriented cylinders can be employed to calculate spectral radiative properties of a spacer [6, 7]; (6) One can use transport approximation without taking into account the details of angular dependence of radiation scattered by fibers [7, 8]; (7) The monodisperse approximation for the spacer's fibers can be used in engineering estimates [7]; (8) The polarization effects can be neglected; (9) The thicknesses of oxide films on both surfaces of the aluminum foil are the same as those in the manufacturing, and no subsequent changes of these oxide layers in space is expected.

The spectral dependences of radiative properties of all substances are taken into account. Nevertheless, the resulting mathematical formulation is rather simple because it is based on balance equations for the spectral radiation fluxes [4]. The model suggested in [3, 4] includes an approximate description of the effect of a thin but dense oxide film formed at the surface of an aluminum foil at normal atmospheric conditions. Infrared optical properties of fused silica have been studied during many years, and the optical constants we need for calculations are well known [9]. The temperature dependences of the optical constants of fused silica and are rather weak and can be neglected in the calculations. The model presented in this section is based on the method of papers [3, 4] generalized to the case of a transient problem for numerous layers of MLI. The resulting equations take into account a set of $L = 21$ isothermal opaque screens with one additional layer corresponding to copper plate placed at the outer side of the MLI. The fibrous spacers located between the first and the last layers are not considered as separate elements of MLI, but their effect on radiative heat transfer is taken into account as described in paper [4]. Thermal radiation from the layer of ceramic fabric is treated as an external radiative flux. There is also a radiative heat transfer between the copper plate and the steel wall of the chamber. This wall was cooled by water to avoid its heating during the experiment. As earlier, we assumed that heat transfer between the layers is a result of the far-field thermal radiation and there is no direct thermal contact between the layers. The resulting mathematical formulation of the problem is as follows:

$$c_l \rho_l \delta_l \frac{dT_l}{dt} = \int_{\lambda_{min}}^{\lambda_{max}} \left(q_{a,l,\lambda} - q_{l,2,\lambda} \right) d\lambda , \quad T_1(0) = T_0 , \quad T_a = T_a(t) \tag{1a}$$

$$c_l \rho_l \delta_l \frac{dT_l}{dt} = \int_{\lambda_{min}}^{\lambda_{max}} \left(q_{l-1,l,\lambda} - q_{l,l+1,\lambda} \right) d\lambda , \quad T_l(0) = T_0 , \quad l = 2,...,20 \tag{1b}$$

$$c_L \rho_L \delta_L \frac{dT_L}{dt} = \int_{\lambda_{min}}^{\lambda_{ma[}} q_{L-1,L,\lambda} d\lambda + \varepsilon_{L,c}^{eff} \sigma \left(T_c^4 - T_L^4 \right), \quad T_L(0) = T_0 \tag{1c}$$

$$c_c \rho_c \delta_c \frac{dT_c}{dt} = \varepsilon_{L,c}^{eff} \sigma \left(T_L^4 - T_c^4 \right) + \varepsilon_{c,s}^{eff} \sigma \left(T_s^4 - T_c^4 \right), \quad T_c(0) = T_0 \quad T_s = T_s(t) \tag{1d}$$

$$0 < t < t_{max}$$

where $\varepsilon_{L,c}^{eff} = \dfrac{\varepsilon_L \varepsilon_c}{\varepsilon_L + \varepsilon_c - \varepsilon_L \varepsilon_c}$ $\varepsilon_{c,s}^{eff} = \dfrac{\varepsilon_c \varepsilon_s}{\varepsilon_c + \varepsilon_s - \varepsilon_c \varepsilon_s}$ are the effective emissivities of the neighboring elements. Index "a*"* refers to the heated fabric, indices "*l"* and "L" refer to the screens of MLI (l = 1,..,6 – for aluminum foil, l = 7,..,20 – for aluminized polymer Upilex, and L – for aluminized Kapton), indices "c" and "s" refer to the copper plate and steel wall of experimental facility, respectively.

Spectral radiative flux through a layer of MLI, which consists of two screens and a spacer made of semi-transparent highly porous fibrous material, is expresses as follows:

$$q_{l,l+1,\lambda} = \frac{f_{l,\lambda} - f_{l+1,\lambda}}{\dfrac{1}{\varepsilon_{l,\lambda}} + \dfrac{1}{\varepsilon_{l+1,\lambda}} + \dfrac{2}{1 + T_\lambda - R_\lambda} - 2} \tag{2}$$

where $\varepsilon_{l,\lambda}, \varepsilon_{l+1,\lambda}$ are the spectral emittances of the screens at temperatures T_l and T_{l+1}, $f_\lambda = \pi B_\lambda(T)$ is the blackbody spectral radiative flux, $B_\lambda(T)$ is the Planck function, R_λ and T_λ are the spectral hemispherical reflectance and transmittance of the spacer.

Both transmittance and reflectance of radiation by highly porous fibrous spacers can be determined on the basis of independent scattering hypothesis and Mie theory for infinite homogeneous cylinders. Characteristic of highly porous fibrous spacer can be determined by the relation:

$$U_\lambda = T_\lambda - R_\lambda = 1 - \frac{4}{\pi}(1-p)\tilde{Q}_{\text{tr}} \tag{3}$$

where p is the surface porosity of a spacer, $\tilde{Q}_{\text{tr}}$ is transport efficiency factor of extinction. The values of efficiency factors for cylindrical particles at arbitrary illumination of fibers are calculated using known relations of Mie theory. It should be noted that model (1)–(3) includes some uncertainties in material properties, And the spectral emittance of heated fabric $\varepsilon_{a,\lambda}$ is the main of them. Therefore, the latter value should be identified to complete the computational model.

3. INVERSE PROBLEMS ALGORITHM

In a general case, the heat transfer is determined by (1) the parameters of interaction with an environment (experimental facility and heater), (2) the radiative heat transfer in MLI, (3) thermal properties, densities and thickness of the MLI layers, as well as by the system's initial temperature. As was noted, the material properties in the model (1)–(3) have some uncertainties in, and the spectral emittance of heated fabric $\varepsilon_{a,\lambda}$ is the main of them. The results of temperature measurements in the cooper slab (1d) can be considered as additional information, which is not necessary to solve direct heat transfer problem.

$$T_c^{\exp}(\tau_m) = f_m, \quad m = \overline{1, M} \tag{4}$$

Strictly speaking, the retrieval of functions $\varepsilon_{a,\lambda}$ is related with to a minimization of the residual functional characterizing the deviation of temperature $T_c(\tau_m)$ calculated for certain estimates of $\varepsilon_{a,\lambda}$ from the measured temperature f_m in the corresponded metric. The following functional can be considered to characterize the least-square deviation of experimental and calculated temperatures:

$$J(\varepsilon_{a,\lambda}) = \int_0^{\tau_{max}} (T_c(\tau) - f(\tau))^2 d\tau \tag{5}$$

To solve the inverse problem, the conjugate gradient method of minimization as the base of iterative regularization method [1] can be used. According to the approach suggested in [2], the unknown coefficient can be approximated by a set of basic functions (in particular, peas-waste functions or B-splines):

$$\varepsilon_{a,\lambda}(\lambda)=\sum_{k=1}^{N} e_k \varphi_k(\lambda) \tag{6}$$

The gradient of the minimized functional is computed using the solution of an adjoint problem:

$$J'_{e_k}=\int_{\lambda_{min}}^{\lambda_{max}} \Psi_l \left(\frac{\varphi_k(\lambda)\varepsilon_{1,\lambda}(1+T_\lambda-R_\lambda)}{(\varepsilon_{1,\lambda}(1+T_\lambda-R_\lambda)+\varepsilon_{a,\lambda}(1+T_\lambda-R_\lambda)+2\varepsilon_{a,\lambda}\varepsilon_{1,\lambda}-2\varepsilon_{a,\lambda}\varepsilon_{1,\lambda}(1+T_\lambda-R_\lambda))} - \right.$$
$$\left. \frac{\varepsilon_{a,\lambda}\varepsilon_{1,\lambda}(1+T_\lambda-R_\lambda)\varphi_k(\lambda)((1+T_\lambda-R_\lambda)+2\varepsilon_{1,\lambda}-2\varepsilon_{1,\lambda}(1+T_\lambda-R_\lambda))}{(\varepsilon_{1,\lambda}(1+T_\lambda-R_\lambda)+\varepsilon_{a,\lambda}(1+T_\lambda-R_\lambda)+2\varepsilon_{a,\lambda}\varepsilon_{1,\lambda}-2\varepsilon_{a,\lambda}\varepsilon_{l1,\lambda}(1+T_\lambda-R_\lambda))^2} \right)(f_{a,\lambda}-f_{1,\lambda})d\lambda \tag{7}$$

where ψ_l is the solution of the following adjoint problem:

$$-c_1\rho_1\delta_1\frac{d\Psi_1}{dt}=\int_{\lambda_{min}}^{\lambda_{max}}\left(\frac{\varepsilon_{a,\lambda}\varepsilon_{+1,\lambda}(1+T_\lambda-R_\lambda)(-)}{(\varepsilon_{1,\lambda}(1+T_\lambda-R_\lambda)+\varepsilon_{a,\lambda}(1+T_\lambda-R_\lambda)+2\varepsilon_{a,\lambda}\varepsilon_{l+1,\lambda}-2\varepsilon_{a,\lambda}\varepsilon_{1,\lambda}(1+T_\lambda-R_\lambda))} - \right.$$
$$\left. \frac{\varepsilon_{1,\lambda}\varepsilon_{l2,\lambda}(1+T_\lambda-R_\lambda)(\Psi_1(\tau)df_{1,\lambda}/dT-\Psi_2(\tau)df_{2,\lambda}/dT)}{(\varepsilon_{2,\lambda}(1+T_\lambda-R_\lambda)+\varepsilon_{1,\lambda}(1+T_\lambda-R_\lambda)+2\varepsilon_{1,\lambda}\varepsilon_{2,\lambda}-2\varepsilon_{1,\lambda}\varepsilon_{2,\lambda}(1+T_\lambda-R_\lambda))} \right)d\lambda,$$
$$\Psi_1(\tau_{\max})=0, \tag{8a}$$

$$-c_l\rho_l\delta_l\frac{d\Psi_l}{dt}=\int_{\lambda_{min}}^{\lambda_{max}}\left(\frac{\varepsilon_{l-1,\lambda}\varepsilon_{l,\lambda}(1+T_\lambda-R_\lambda)(\Psi_{l-1}(\tau)df_{l-1,\lambda}/dT-\Psi_l(\tau)df_{l,\lambda}/dT)}{(\varepsilon_{l,\lambda}(1+T_\lambda-R_\lambda)+\varepsilon_{l-1,\lambda}(1+T_\lambda-R_\lambda)+2\varepsilon_{l,\lambda}\varepsilon_{l-1,\lambda}-2\varepsilon_{l,\lambda}\varepsilon_{l-1,\lambda}(1+T_\lambda-R_\lambda))} - \right.$$
$$\left. \frac{\varepsilon_{l,\lambda}\varepsilon_{l+1,\lambda}(1+T_\lambda-R_\lambda)(\Psi_l(\tau)df_{l,\lambda}/dT-\Psi_{l+1}(\tau)df_{l+1,\lambda}/dT)}{(\varepsilon_{l+1,\lambda}(1+T_\lambda-R_\lambda)+\varepsilon_{l,\lambda}(1+T_\lambda-R_\lambda)+2\varepsilon_{l,\lambda}\varepsilon_{l+1,\lambda}-2\varepsilon_{l,\lambda}\varepsilon_{l+1,\lambda}(1+T_\lambda-R_\lambda))} \right)d\lambda,$$
$$\Psi_l(\tau_{max})=0\,,\ l=2,...,20 \tag{8b}$$

$$-c_L\rho_L\delta_L\frac{d\Psi_L}{dt}=\int_{\lambda_{max}}^{\lambda_{min}}\left(\frac{\varepsilon_{L-1,\lambda}\varepsilon_{L,\lambda}(1+T_\lambda-R_\lambda)(\Psi_{L-1}(\tau)df_{L-1,\lambda}/dT-\Psi_L(\tau)df_{L,\lambda}/dT)}{(\varepsilon_{L,\lambda}(1+T_\lambda-R_\lambda)+\varepsilon_{L-1,\lambda}(1+T_\lambda-R_\lambda)+2\varepsilon_{L,\lambda}\varepsilon_{L-1,\lambda}-2\varepsilon_{L,\lambda}\varepsilon_{L-1,\lambda}(1+T_\lambda-R_\lambda))} \right)d\lambda$$
$$+4\varepsilon_{L,c}^{eff}\sigma(T_c^3-T_L^3),$$
$$\Psi_L(\tau_{max})=0 \tag{8c}$$

$$-c_c\rho_c d_c\frac{d\psi_c}{d\tau}=4\varepsilon_{L,c}^{eff}\sigma(T_L^3-T_c^3)+4\varepsilon_{c,s}^{eff}\sigma(T_s^3-T_c^3)+2(T_c(\tau)-f(\tau)), \qquad \Psi_c(\tau_{\max})=0 \tag{8d}$$

4. COMPUTATIONAL RESULTS

An application of inverse problem methods for heat transfer problems, is related with a specific testing of the developed algorithms. The most universal approach hereby is a computational experiment, which is made in the following way: first a direct heat transfer problem in the specimen should be solved, on the assumption that all characteristics of material are known. Using the obtained values of temperature in the supposed points of thermosensors installation, then "experimental" data necessary for solving an inverse problem are formed, and after that an inverse problem on determining of $\varepsilon_{a,\lambda}$ is solved. Random errors in the "experimental" data are formed as follows

$$f(\tau) = \tilde{f}(\tau)\left(1 + \delta_f \omega(\tau)\right) \tag{9}$$

where $\tilde{f}(\tau)$ is the exact value, ω is a random value of normal distribution with a mean value equal 0.0 and a dispersion equal 1.0, $\delta_f = 0.05$ is a relative error. The computational results at conditions of experimental heating are presented in Fig. 5. The emissivities of oxidized copper plate surface and steel surface were taken equal to 0.6 and 0.45, respectively. As to parameters of fibrous spacers, the fiber radius was taken equal to $a = 3$ μm and the surface porosity – $p = 0.8$. The wavelength range from $\lambda_{min} = 2$ μm to $\lambda_{\max} = 20$ μm was used while integrating over the spectrum since this range makes the main contribution to the integral radiative flux.

A comparison of the calculated and "measured" temperatures of copper slab as a result of inverse problem solving for different approximations (6) is presented in Fig. 6 and in Table 1. The estimated values of $\varepsilon_{a,\lambda}$ for different approximation are presented in Fig.7. As one can expect, the minimal set of the approximation parameters provides the best accuracy and stability of inverse problems solving. Though in the case of approximation by peace-waste functions with N=2 we used the a-priori information about the spectral boundary of two-band model of spectral properties of quartz fibers [10] (with the "boundary" wavelength about 6.5 μm), but the estimate of this value can be obtained from other approximations (Fig. 7, curves 2-4).

Table 1: The deviation of the calculated temperatures and measured temperatures

Approximation	Least-squares temperature deviation (K)	Temperature deviation (%)	Maximum deviation (K)	Maximum deviation (%)
1	1.24	4.1	2.5	7.1
2	1.16	4.3	2.3	7.5
3	1.21	4.7	2.4	6.2
4	0.37	2.4	1.2	4.3

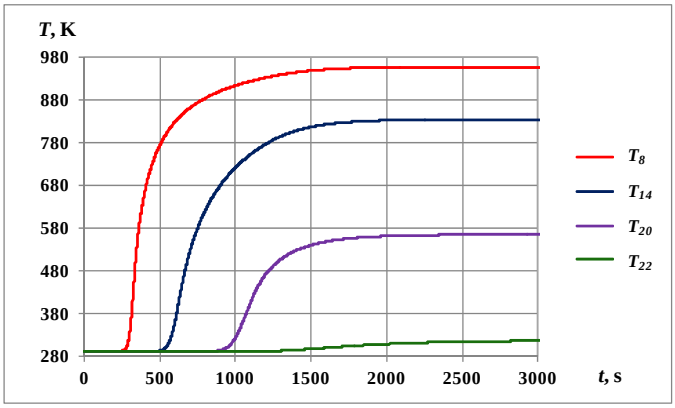

Figure 5: Temperature of MLI layers calculated for the stages of initial heating: the numbers of MLI layers are specified in panels of the figure.

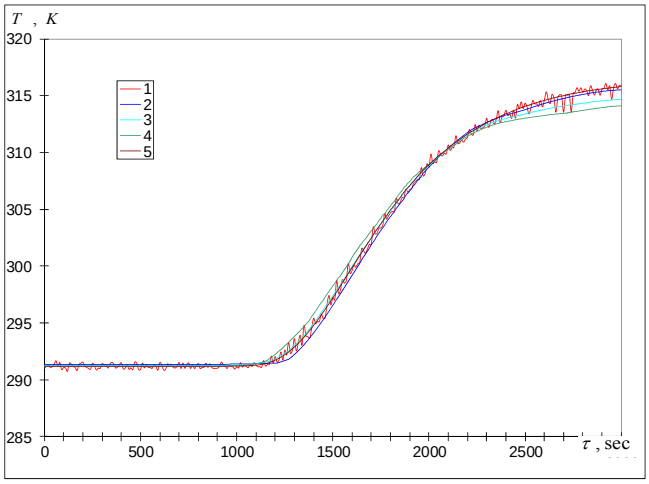

Figure 6: Comparison of theoretical predictions and experimental data for temperature of copper plate: 1 – "experimental", 2–4 – aproximations (2) by cubic B-splines at N=5, (3) by cubic B-splines at N=3, (4) – by peace-waste functions at N=36, (5) by peace-waste functions at N=2.

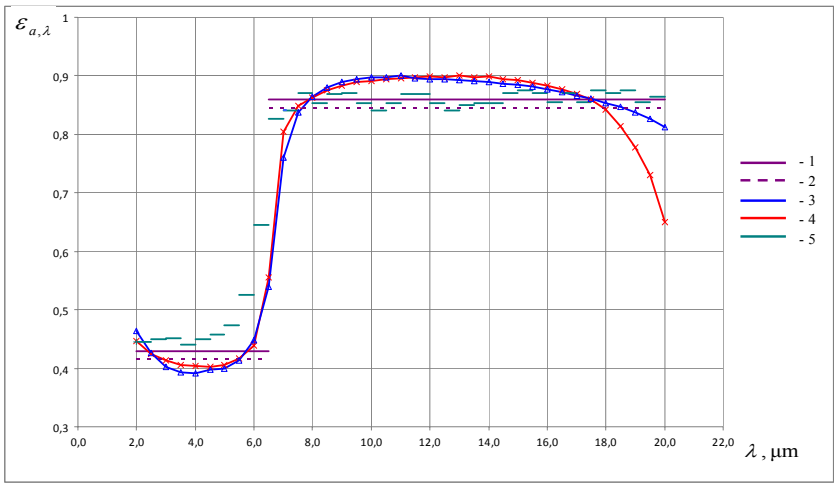

Figure 7: Reconstruction of $\varepsilon_{a,\lambda}$: 1 – "exact" value, 2–5 – estimations using (2) cubic B-splines at N=5, (3) cubic B-splines at N=3, (4) peace-waste functions at N=36, (5) peace-waste functions at N=2.

5. CONCLUSIONS

An identification procedure for mathematical model of the multilayer thermal insulation (MLI) of space vehicles with the use of the MLI sample of the BP-Colombo satellite (ESA) showed that a theoretical model developed recently by the authors can be used to estimate thermal properties of the insulation at conditions of space vacuum. The above comparison enables us to use the developed method to analyze wide-range spectral properties of the MLI. A further study of the external pressure effect on radiative transfer in single layers of MLI is expected to be interesting both theoretically (to

observe possible near-field effects) and practically (to predict variation of the heat shielding properties of the MLI at conditions of a planetary atmosphere).

ACKNOWLEDGMENTS

The authors are grateful to the Russian Foundation for Basic Research for the financial support of this study (grant 13-08-00022-a). This work was also supported by the Russian president grant for Scientific Team NSh- 6343.2014.8.

REFERENCES

[1] Alifanov, O.M., *Inverse Heat Transfer Problems*, Springer-Verlag, Berlin, 1994.

[2] Alifanov, O.M., Nenarokomov, A.V., and Gonzalez, V.M., *Study of multilayer thermal insulation by inverse problems method*, Acta Astronautica, 65, (2009).

[3] Gritsevich, I.V., Dombrovsky, L.A., and Nenarokomov, A.V., *Heat transfer by radiation in a vacuum thermal insulation of space vehicles*, Therm. Proc. Eng., 5(1), (2013), pp. 12-21. (in Russian)

[4] Gritsevich, I.V., Dombrovsky, L.A., and Nenarokomov, A.V., *Radiative transfer in vacuum thermal insulation of space vehicles*, Comput. Therm. Sci., 2014, in press.

[5] Tien, C.L. and Drolen, B.L., *Thermal radiation in particulate media with dependent and independent scattering*, in "Annual Review of Numerical Fluid Mechanics and Heat Transfer", New York: Hemisphere, (1987), v. 1, pp. 1-32.

[6] Bohren, C.F. and Huffman, D.R., *Absorption and Scattering of Light by Small Particles*, New York: Wiley, (1983).

[7] Dombrovsky, L.A. and Baillis, D., *Thermal Radiation in Disperse Systems: An Engineering Approach*, New York: Begell House, (2010).

[8] Dombrovsky, L.A., *The use of transport approximation and diffusion-based models in radiative transfer calculations*, Comput. Therm. Sci., (2012), 4(4), pp. 297-315.

[9] Kitamura, R., Pilon, L., and Jonasz, M., *Optical constants of silica glass from extreme ultraviolet to far infrared at near room temperatures*, Appl. Opt., (2007), 46(33), pp. 8118-8133.

[10] Dombrovsky, L.A., *Quartz-fiber thermal insulation: Infrared radiative properties and calculation of radiative-conductive heat transfer*, ASME J. Heat Transfer, (1996) 118(2), pp. 408-414.